Pharm Res (2012) 29:1949–1959
DOI 10.1007/s11095-012-0723-7

RESEARCH PAPER

Treatment of Experimental Brain Metastasis with MTO-Liposomes: Impact of Fluidity and LRP-Targeting on the Therapeutic Result

Andrea Orthmann • Reiner Zeisig • Regine Süss • Dorothea Lorenz • Margit Lemm • Iduna Fichtner

Received: 5 January 2012 / Accepted: 24 February 2012 / Published online: 8 March 2012

ABSTRACT

Purpose To test targeted liposomes in an effort to improve drug transport across cellular barriers into the brain.

Methods Therefore we prepared Mitoxantrone (MTO) entrapping, rigid and fluid liposomes, equipped with a 19-mer angiopeptide as ligand for LDL lipoprotein receptor related protein (LRP) targeting.

Results Fluid, ligand bearing liposomes showed *in vitro* the highest cellular uptake and transcytosis and were significantly better than the corresponding ligand-free liposomes and rigid, ligand-bearing vesicles. Treatment of mice, transplanted with human breast cancer cells subcutaneously and into the brain, with fluid membrane liposomes resulted in a significant reduction in the tumor volume by more than 80% and in a clear reduction in drug toxicity. The improvement was mainly depended on liposome fluidity while the targeting contributed only to a minor degree. Pharmacokinetic parameters were also improved for liposomal MTO formulations in comparison to the free drug. So the area under the curve was increased and $t_{1/2}$ was extended for liposomes.

Conclusion Our data show that it is possible to significantly improve the therapy of brain metastases if MTO-encapsulating, fluid membrane liposomes are used instead of free MTO. This effect could be further enhanced by fluid, ligand bearing liposomes.

KEY WORDS brain metastases · LRP· targeting · transcytosis · uptake

ABBREVIATIONS

BBB	blood–brain barrier
DMEM	Dulbecco's Modified Eagle Medium
FCS	foetal calf serum
LDL	low-density lipoprotein
LRP	LDL-lipoprotein receptor related protein
LUV	large unilamellar vesicles
MDCK	Madin-Darby canine kidney
MTO	mitoxantrone
PIT	post insertion technology
RTV	relative tumor volume

INTRODUCTION

Brain metastases are the most serious neurological complication related to cancer. Systemic treatment with anticancer drugs for primary brain tumors and metastases in the brain often fail due to the highly efficient blood–brain barrier (BBB) formed by endothelial linings of small capillaries in

Electronic supplementary material The online version of this article (doi:10.1007/s11095-012-0723-7) contains supplementary material, which is available to authorized users.

A. Orthmann · M. Lemm · I. Fichtner
Experimental Pharmacology
Max Delbrück Center for Molecular Medicine
Robert-Rössle-Str. 10
13125 Berlin-Buch, Germany

R. Zeisig (✉)
Experimental Pharmacology & Oncology Berlin-Buch GmbH
Robert-Rössle-Str. 10
13125 Berlin-Buch, Germany
e-mail: Reiner.Zeisig@epo-berlin.com

R. Süss
Department of Pharmaceutical Technology and Biopharmacy
Albert-Ludwigs University
Stefan-Meier-Str. 19
79104 Freiburg, Germany

D. Lorenz
Cellular Imaging
Leibniz-Institut für Molekulare Pharmakologie (FMP)
Robert-Rössle-Str. 10
13125 Berlin, Germany

the brain. This multi-component tight cell barrier is responsible for the maintenance of normal brain homeostasis and allows only necessary nutrient to penetrate into the brain parenchyma, whereas harmful compounds including anticancer drugs are efficiently blocked (1,2).

The entrapment of drugs into nanoparticles (3,4) and liposomes (5,6) was shown to be able to overcome this problem. Knowledge of nanoparticle technology has significantly improved and can be applied to provide better drug delivery to different target sites (6), including the brain parenchyma (7). Based on our long-standing experiences with liposomes as a powerful tool to improve anticancer therapy, we were interested to apply this technology for the treatment of brain malignancies.

In our previous study we investigated more than 25 different liposomal formulations concerning the impact of their membrane properties on uptake and transcytosis. It was found that fluid liposomes, L_{fluid}, containing the helper lipids DOPE and OPP as additional components to the basic lipid PC had the best cellular uptake and transcytosis across a tight cellular barrier *in vitro* (8).

It was the aim of the current study to equip these liposomes with a peptide at the surface to target a specific receptor expressed on the BBB in order to further improve drug transport into the brain. These liposomes were then compared with similar ligand bearing liposomes with a higher rigidity and with the corresponding ligand free vesicles *in vitro* and *in vivo*.

Only a few targets on the endothelial BBB have been studied to enable receptor-mediated nanocarrier transport to the brain (for reviews see (9–11)), including the transferrin receptor (7,12), insulin receptor (13), folate receptor (14), epidermal growth factor receptor (15), and the low-density lipoprotein (LDL) receptor (16).

We selected the LDL receptor related protein (LRP) as target. This protein belongs to the LDL receptor family, a group of approximately ten tissue dependent cell surface receptors (17) with LDL as ligand. LRP is expressed by cerebral endothelial cells and neuronal cells such as astrocytes, and has a high endocytotic activity (18). LDL binds with its apolipoprotein B100 (ApoB100) to the LRP as a spherically shaped structure (19).

Intensive work has been done by the group of Beliveau (16,20) to establish a peptide platform for targeted CNS therapeutics. Angiopeptide (angiopep), a short peptide sequence derived from the LRP ligand aprotinin, consists of 19 amino acids. Among different sequences, angiopep-2 was identified to be responsible for the most efficient LRP binding. Beliveau's group used this peptide to conjugate three molecules of paclitaxel to the peptide. This new drug delivery system, called ANG1005, was shown to transport the drug across the BBB very effectively (21). New conjugates were recently introduced, carrying doxorubicin or etoposide (22).

We used the angiopep-2 as ligand and conjugated it to the surface of fluid membrane liposomes containing Mitoxantrone (MTO). To our knowledge, this is the first time that a liposomal system targeting the LRP was used for drug transport across cellular barriers such as the BBB. These targeted liposomes were physico-chemically characterized and tested *in vivo* for their therapeutic effect in an experimental brain metastasis model of human breast cancer, recently established in our lab.

We demonstrated that the use of fluid membrane liposomes after surface modification with the angiopeptide sequence improved the therapeutic potential of a cytotoxic drug and contributes to an improved treatment of experimental brain metastases.

MATERIALS AND METHODS

Materials

Liposomal components, chemicals solvents and cell culture material were obtained from suppliers as described recently (8). Octadecyl-1,1-dimethylpiperidin-1-ium-4-yl phosphate (OPP, Perifosine) was a generous gift from Dr. Hilgard (ASTA Medica, Frankfurt, Germany) and phosphatidylcholine (PC-E) from Lipoid (Ludwigshafen, Germany). 1,2 Dioleyl-sn-glycero-3-phosphoethanolamine was a product of Sigma – Aldrich, Taufkirchen, Germany.

Ligand and model compounds: anchor ligand Chol-19-mer-peptide (**1**), labeled ligand 5-Fluo-19-mer peptide (**2**) and the anchor model Chol-5-Fluo derivative (**3**) were synthesized by Biosyntan GmbH (Berlin, Germany) by Fmoc/But-strategy (23). The configuration, properties and application of ligands used in this study are summarized in Table I. Purification was performed by high performance liquid chromatography. Compounds were obtained in 60–70% (**1**), 90–95% (**2**) or 90% (**3**) purity. Lyophilisates were stored at −20°C in dry form until use.

Liposome Preparation

Composition and properties of control and ligand modified liposomes used in this study are summarized in Table II. Large unilamellar vesicles (LUV) were prepared by lipid film hydration in combination with extrusion technology as described recently (8) using filter with a pore size of 200 nm to obtain rigid (L_{rigid}) and more fluid formulations (L_{fluid}) with a diameter smaller than 200 nm. Hydration was performed using a) phosphate buffered saline (PBS, pH 7.5); b) calcein solution (50 mM, pH 7.5) or c) ammonia citrate buffer (300 mM, pH 7.4) to obtain liposomes for optimization of post insertion technology (PIT), for *in vitro* investigations and for MTO-loading for *in vivo* studies, respectively.

Table I Ligands Used to Modify the Surface of Liposomes

Comp.	Code	Structure	Molecular weight theor./found [g/mol]	Use
1	Chol-19-mer-peptide	CHSU-TFFYGGSRGKRNNFKTEEY-amid x TFA	2769.3/2770.2	Anchor ligand
2	5-Fluo-19-mer-peptide	5-Fluo-Ahx-TFFYGGSRGKRNNFKTEEY-amid x TFA	2772.0/2772.7	Labelled ligand, FACS
3	Chol-5-Fluo derivative	CHSU-PEG2-PEG2-Lys(5Fluo)-amid x TFA	1262.6/1263.9–1266.1	Anchor model

CHSU Cholesteryl-hemisuccinat; *PEG* Polyethylenglycol; *Lys* Lysine; *5-Fluo* 5-Carboxyfluorescein; *TFA* Trifluoroacetic acid; *Ahx*: 6-aminohexancabon acid
Individual amino acids are indicated by one-letter abbreviation.

Liposomes containing calcein were finally separated from non encapsulated material by size exclusion technology using sephadex G50 columns.

Remote loading of MTO into LUV, prepared in ammonia citrate buffer was done as described before (24), with minor modifications. The external ammonium citrate buffer was exchanged against PBS using sephadex G50 columns. The resulting liposomal suspension was heated to 60°C in a water bath before MTO (2 mg/ml) in a ratio of 1:1 (v/v) was added. After short vortexing, the suspension was incubated for 10–30 min at 60°C, followed by soft agitation at room temperature for 12 h. Non encapsulated MTO was removed from liposomes by dialysis using a Spectra/Por® dialysis membrane (MWCO 6000–8000).

Post Insertion Technology (PIT)

To conjugate the 19-mer peptide **1** to the surface of liposomes obtained after step 2, PIT, was used as described recently (25). The PIT method was first optimized before LRP ligand bearing vesicles (L-LG) were prepared as follows: The fluorescently labeled cholesterol-anchor molecule **3** was solved in distilled water (2 mg/ml) and was mixed with the liposome suspension to obtain mixtures with 1 to 5 mol% of **3**, compared to the total lipid (TL). This mixture was incubated at 25°C to 70°C for 15, 30, 60 min or over night under shaking at 700 rpm. Free **3** was separated from the liposomes by size exclusion chromatography using Centri Spin-10® sepharose columns. The liposome fraction in the void volume was collected for lipid and fluorescence analysis.

Ligand bearing liposomes for *in vitro* and *in vivo* experiments were prepared in a similar way by using the following optimal conditions: 2 mol% of the Chol-19-mer-peptide **1** were mixed with 7–13 μmol TL liposomes and incubated over night at 28°C. Liposomes for *in vivo* experiments were additionally extruded through 0.4 μm extrusion filters prior to application.

Liposome Characterization

Vesicle size determination was carried out by dynamic light scattering (PCS) measurements with a N5 Submicron Particle Size Analyzer (Beckman Coulter Electronic, Hialeath, FL).

Table II Liposome Properties

Code	Surface and loading modification		Total lipid	Size[a]	PI[b]	Content	
	Ligand	Load	mean ± S.D. [mM]	mean ± S.D. [nm]		Calcein [mmol/mol TL]	MTO [μg/ml]
L_{rigid}	–	Calcein	10.5 ± 1.0	128 ± 6	0.17 ± 0.11	98.4 ± 5.1	–
	–	MTO	7.6 ± 1.3	109 ± 2	0.21 ± 0.03	–	712.1 ± 42.7
L_{rigid}-LG	Chol-19-mer-peptide	Calcein	13.0 ± 0.5	139 ± 2	0.27 ± 0.03	66.4 ± 1.8	–
	Chol-19-mer-peptide	MTO	5.0 ± 0.5	111 ± 1	0.16 ± 0.07	–	551.4 ± 18.1
L_{fluid}	–	Calcein	12.4 ± 0.6	125 ± 2	0.22 ± 0.09	82.6 ± 2.3	–
	–	MTO	8.4 ± 1.2	103 ± 1	0.13 ± 0.05	–	739.1 ± 56.9
L_{fluid}-LG	Chol-19-mer-peptide	Calcein	11.2 ± 0.0	122 ± 4	0.22 ± 0.02	73.7 ± 2.6	–
	Chol-19-mer-peptide	MTO	5.6 ± 0.1	103 ± 0	0.14 ± 0.03	–	602.9 ± 65.1

[a]: Unimodal diameter;

[b]: Polydispersity index (varied between 0: completely monodisperse and 1: polydisperse)

L: Liposome LG: Ligand MTO: Mitoxantrone PI: Polydispersity index Chol-19-mer-pepide: Anchor ligand **1** from Table I

Composition: PC (Phosphatidylcholine) CH: (Cholesterol) DCP: (Dicetylphosphate) OPP: (Octadecyl-1,1-dimethylpiperidin-1-ium-4-yl phosphate) DOPE: (Dioleylphosphatidylethanolamine), molar ratio:70:30:10:0:0 (L_{rigid} and L_{rigid}-LG) and 50:30:10:20:20 (L_{fluid} and L_{fluid}-LG)

Content Quantification: Total lipid concentration was calculated according to the content of the basic lipid PC determined by HPTLC as described recently (26). The calcein content in liposomes was determined by fluorescence measurements in microtiter plates (FluoroNunc™ MaxiSorp Surface) with an Infinite M200 plate reader (Tecan, Crailsheim, Germany) at F_{ex} 485 nm and F_{em} 538 nm. MTO concentration in liposomes was measured in a micro plate reader at 610 nm. Concentration of calcein and MTO were calculated from the standard curves obtained with the free compounds.

Cryotransmission Electron Microscopy (Cryo-TEM)

Samples were plunged-frozen onto glow discharged holey carbon grids (Quantifoil Micro Tools, Jena, Germany) in liquid ethane using a Vitrobot (Vitrobot MarkIV, FEI, Eindhoven, The Netherlands). Temperature was set to 22°C, the relative humidity to 100%. The vitrified grids were mounted into a Gatan cryo-transfer holder (Gatan 626, Gatan Inc. Pleasanton, USA) and introduced into a Tecnai F20 electron microscope (FEI), operated at 200 kV. Samples were imaged at −170°C using standard low-dose imaging conditions. Images were acquired at a magnification of 25 000 and with an underfocus of 4 or 6 µm on a 2kx2k CCD camera (894 Ultrascan 1000, Gatan Inc., Pleasanton, USA).

Cell Culture

Madin-Darby canine kidney cells (MDCK; ECACC, no. 00062107; Wiltshire, UK) were cultured in Dulbecco's Modified Eagle Medium, supplemented with 1% L-glutamine, 7 g/l NaHCO3, 1 g/l Glucose and 10% heat-inactivated foetal calf serum (FCS). Mouse brain endothelial cells (bEnd.3, ATCC, CRL-2299, USA) were cultured in DMEM with 4.5 g/l Glucose and 10% FCS. Human glioblastoma cells (U373 MG; ATCC, HTB-17) and human mammary carcinoma cells (MT-3, WONZ, Russia (27) were cultured in RPMI 1640 media with 10% FCS.

Cellular Uptake

Uptake of liposomes was determined as described recently (8). Briefly: $3*10^5$ cells/well, cultured in a 24-well microtiter plate, were incubated with 600 µl calcein loaded liposomes in serum free media (75 nmol total lipid/ml) for different time periods at 37°C. Unspecific uptake was determined under similar conditions after incubation for 15 min at 4°C. Cellular calcein concentration was determined by fluorescence measurement after cell lysis with Ripa-buffer. All experiments were performed in triplicate in three independent experiments.

Transcytosis

Transcytosis was determined as described recently (8) as follows: $1*10^5$ MDCK-cells, seeded on a permeable cell culture insert of a transwell system (Millipore; 0.2 µm pore size, diameter, 0.6 cm^2, 0.2% collagen coated), were used after a tight monolayer was obtained. Cells in the apical chamber of the transwell system were incubated with 400 µl nutrient deficient DMEM containing the liposomes (75 nmol total lipid/ml) at 37°C for 24 h. Calcein concentration in the basal media and in cells was determined by fluorescence measurement directly (basal media) or after lysis (cells). Three independent experiments were performed, each done in triplicate.

Experimental Metastasis *In Vivo*

All animal experiments were performed according to the German Animal Protection Law, to "Principles of Laboratory Animal Care" (NIH publication #85-23, revised in 1985) and with approval of the local responsible authorities.

Adult female NMRI:nu/nu mice were obtained from Taconic Europe (Lille Skensved, Denmark). The animals were housed under pathogen-free conditions in individually ventilated cages under standardized environmental conditions (22°C room temperature, 50 ± 10% relative humidity, 12 h light–dark rhythm). They received autoclaved food and bedding (Ssniff, Soest, Germany) and acidified (pH 4.0) drinking water *ad libitum*.

Human MT3-breast carcinoma cells were transplanted into the brain ($5*10^3$ cells) and subcutaneously into the left flank ($5*10^6$ cells) of each mouse. Animals were randomly assigned into experimental groups with 8 mice each. Intravenous treatment with MTO-containing liposomes or with free MTO, each at a dose of 4 mg/kg was performed at day 3, 7 and 10. Control mice received saline solution in the same schedule. Tumor diameter of the s.c. tumor was measured twice a week with a caliper. Tumor volumes were calculated according to $V = \left(\text{length} * (\text{width})^2\right)/2$. For calculation of the relative tumor volume (RTV) of the s.c. tumor, the tumor volumes at each measurement day were related to the day of first treatment. Body weight was determined twice a week. Mice were sacrificed when the mice of the control groups showed first signs of extracerebral tumors at place of cell injection. Brains were isolated, snap-frozen and cryo-sections were prepared. The size of the tumor area was determined after staining with cresyl violet followed by microscopic identification (Zeiss Axioskop, equipped with the 3CCD video camera Sony Power Head) and calculated with the software IQ Easy Measure® (Version 1.4.1). Data were obtained from two independently performed experiments and are given as mean values ± S.D (n: 5–16).

Pharmacokinetic Analysis

Pharmacokinetic (PK) parameters were determined using s.c. and intracerebral tumor bearing female NMRI:nu/nu mice. MT-3 bearing mice were treated with a single dose of 5 mg MTO/kg i.v. in solution or encapsulated in L_{fluid} or L_{fluid}-LG liposomes and randomized into groups with 3 mice each. At predefined time points (5′, 15′, 30′, 1 h, 2 h, 4 h, und 48 h) blood was taken from retro-orbital sinus after iso-flurane anesthesia, before the mice were sacrificed by cervical dislocation. Tumors and different organs were isolated and snap frozen until analysis.

Samples were processed accordingly to Johnson (28) and quantification was performed by HPLC analysis using a NUCLEOSIL® C18 column, run with acetonitrile:ammonia formiat (160 mM) and hexansulfonic acid (25 mM) (33:67, v:v), equilibrated with formic acid at pH 2.7, as isocratic phase. MTO was detected at 610 nm and the concentration was calculated in relation to a standard curve of MTO. Each result represents the mean value for three mice, determined in duplicate.

PK data were finally calculated using the Win-Nonlin program from Scientific Consulting Inc., Apex, NC, USA. PK parameters for plasma distribution were calculated based on a two-compartment model for a single i.v. bolus injection.

Statistical Evaluation

All data are expressed as mean value ± standard deviation (SD). Statistical comparisons of *in vitro* data were performed with the unpaired Student's *t*-test for two populations, whereas statistical evaluation of *in vivo* data was performed with the *U*-test of Mann and Whitney using the Windows program STATISTICA 6. Differences were considered to be significant at $p<0.05$.

RESULTS

We prepared fluid and rigid, MTO-loaded membrane liposomes, which were additionally equipped on their surface with the angiopeptide sequence as ligand for LRP targeting in order to investigate the transport across a tight cellular barrier and to determine the therapeutic potential of these targeted vesicles.

Liposome Preparation

Ligand equipped vesicles were prepared in a three-step process. First, rigid and fluid LUV (L_{rigid} and L_{fluid}) were prepared by lipid film hydration and subsequent extrusion technology as described previously (8). Fluidity of the liposome membrane was already characterized in our previous study by EPR measurements (8). Compared to rigid liposomes L_{rigid}, which were also included in the study for control reasons, the membrane of L_{fluid} liposomes had a shorter relaxation time close to the surface and also in the middle of the membrane (data not shown). This was also reflected in the ordering parameters for three domains which could be distinguished. In all domains the ordering parameter S was smaller in liposomes L_{fluid} than in L_{rigid} (Table III).

The next step was the encapsulation of the drug MTO by remote loading technology (24). These vesicles had a size smaller than 200 nm to reduce uptake by the MPS (34,35) and the size distribution was narrow with a PI less than 0.30, demonstrating that homogeneous formulations were prepared. In the last step, LUV with entrapped MTO were surface modified with the derivative **3** or with the 19-mer peptide **1** (Table I) by PIT as described recently (25).

In order to identify optimal conditions to equip the liposomes with ligand **1**, optimization experiments were performed using the fluorescently labeled cholesteryl derivative **3**, which was designed to mimic the ligand molecule **1**. The molar ratio, incubation temperature (Fig. 1), and time of incubation were modified. The optimal conditions to bind the maximum amount of ligand **3** were finally assigned to the angiopep cholesterol derivative **1**. We decided to use 2 mol% of the peptide, because incubation with higher concentration of ligand **3** (3 and 5 mol%) did not further enhance binding efficacy. Figure 1 shows that the best ligand binding was obtained at 70°C, but we observed liposome destruction at this temperature. To prevent this, we finally used an incubation temperature of only 28°C and extended the time of incubation to 12 hours to obtain sufficient ligand binding. Vesicles with approximately 84% of the ligand could finally be preprared. That amounts to approximately 17 mmol ligand/mol total lipid, as deduced from results obtained with the model ligand. We did not quantify this for the cholesterol-conjugated original peptide sequence, because the uptake experiments indicated a sufficient binding of the ligand bearing liposomes in our cellular system. With this

Table III Ordering Parameter S from Electron Paramagnetic Resonance Measurements for Rigid (L_{rigid}) and Fluid (L_{fluid}) Liposomes

Domain	L_{rigid}	L_{fluid}
D1 (disordered domain)	0.15 (31%)*	0,10 (28%)
D2 (ordered domain)	0.48 (38%)	0.35 (28%)
D3 (domain between D1 and D2)	0.21 (28%)	0.02 (44%)

Shown are the ordering parameters S for three different domains which were distinguished by EPR measurements of liposomes, modified with the lipophilic spin probe MeFASL(10,3), using a X-band EPR spectrometer Bruker ESP 300 at 25°C as described recently (44). Spectrometer settings were: microwave power 10 mW, modulation amplitude 0.1 mT, frequency of modulation 100 kHz, and number of scans for each spectrum was seven.

*: S value (proportion of the specific domain in the membrane).

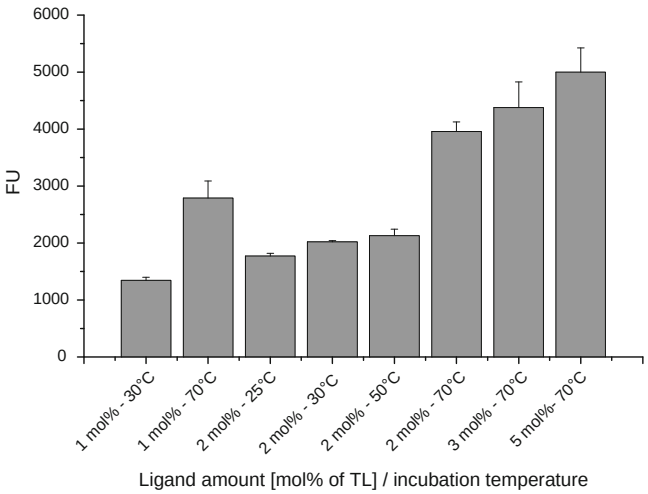

Fig. 1 Effect of concentration and of incubation temperature on ligand insertion into liposomal surface. Pre-formulated liposomes L_{fluid} (see Tables II and III) were incubated at indicated temperatures with 1–5 mol% of the fluorescence-labeled cholesteryl-derivative **3** for 30 min. Fluorescence of liposomes was measured at F_{EX} 485 nm and F_{EM} 517 nm. Data represent the mean fluorescence units (FU) ± S.D. of 2 experiments, each done in triplicate.

preparation method, liposomes at a concentration of 5–8 mM TL, which contained between 712 and 739 µg MTO/ml for ligand-free formulations and 551–603 µg MTO/ml for ligand bearing liposomes were finally obtained (Table II). This corresponds to 60% MTO encapsulation efficacy, resulting in a drug concentration of 0.6 mg/ml (Table II), which is sufficient for animal treatment according to the SOLAS recommendation (29).

All liposomes revealed good storage stability for at least 160 days in terms of stable size (Supplementary Material, Figure S1) and size distribution as analyzed by PCS measurements. No remarkable marker release was observed (data not shown).

In comparison to calcein loaded liposomes the encapsulation of MTO reduced the size of the vesicles by approximately 15%–18% for rigid and fluid liposomes, respectively (Table II).

The precipitated drug can be seen in all MTO encapsulating liposomes (Fig. 2). The insertion of the ligand resulted in complexes of unilamellar liposomes and elongated structures (not shown) and an additional extrusion step through 0.4 µm pore size filters was necessary to obtain the homogeneous formulations shown in Fig. 2c (L_{rigid}LG) and d (L_{fluid}LG). These formulations were used for animal studies.

Cellular Uptake

We confirmed data from the previous study obtained with MDCK cells. Figure 3 shows the amount of marker found in the cells after 24 h. L_{fluid} liposomes showed significantly greater uptake than L_{rigid} by MDCK and bEnd.3 ($p<0.001$).

The presence of ligand **1** at the liposomal surface further enhanced the uptake by a factor of 2.6 (MDCK), 4.0 (bEnd.3), 7.8 (U373 MG), and 2.9 (MT-3) in comparison to ligand free liposomes. Best results in all cells investigated were obtained with L_{fluid}-LG, leading to a maximum uptake of 257 nmol calcein/well by U373 MG cells, which represents an increase of more than 9-fold compared to the control formulation L_{rigid}.

Transcytosis

Between 1.4 and 5.1% of liposomal calcein added to the donor part of the transwell system were transcytozed (Fig. 4).

As recently reported (8), fluid vesicles (L_{fluid}) were transcytozed to a greater degree than rigid liposomes (L_{rigid}). The presence of ligand **1** enhances transcytosis 1.4-fold and 1.8-

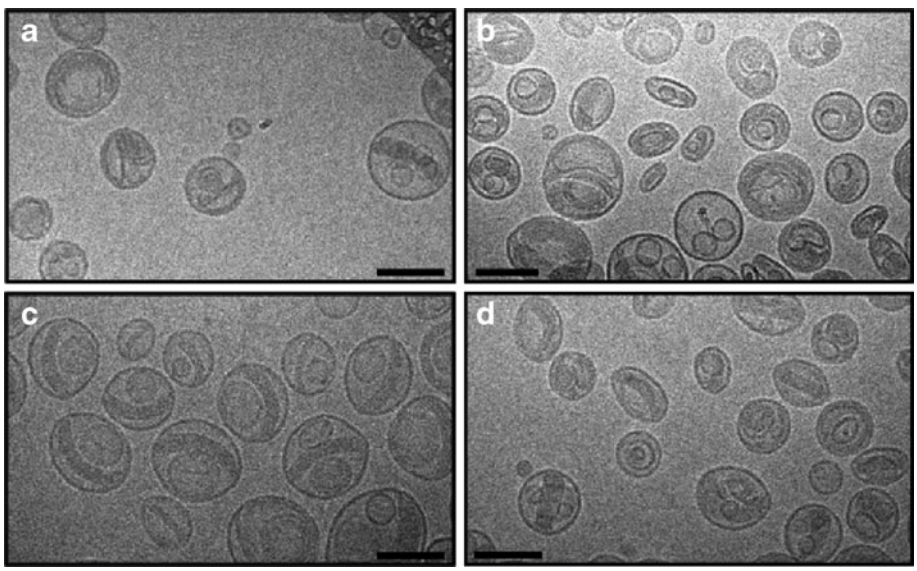

Fig. 2 Cryo-TEM characterization of liposomes. Cryo-TEM pictures show liposomes containing MTO. Micrographs in the top panels represent liposomes without ligand (**a**) L_{rigid} and (**b**) L_{fluid}; while the lower panels show ligand-coupled liposomes (**c**) L_{rigid}-LG and (**d**) L_{fluid}-LG. Bars in the micrographs indicate 100 nm.

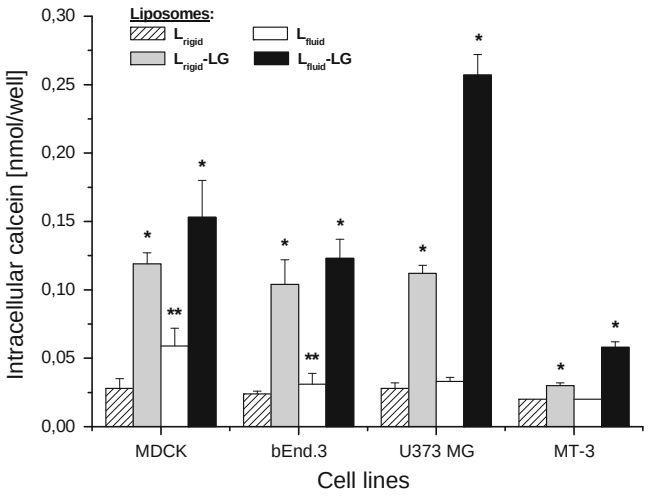

Fig. 3 Cellular uptake of calcein loaded ligand-free and ligand bearing liposomes. Uptake of liposomal calcein by epithelial MDCK, endothelial bEnd.3, glioma U373 MG and breast cancer MT-3 cells was investigated. Cells ($3*10^5$) were incubated with liposomes in serum free DMEM for 24 h at 37°C. After washing, cells were disrupted and the calcein concentration was determined by fluorescence measurement as described in Materials and Methods. Results are corrected for unspecific uptake. All experiments were performed in triplicate in three independent experiments. *: Data are significantly different to corresponding ligand-free liposomes and to other ligand bearing liposomes ($p < 0.0001$); all data are significantly different to each other ($p < 0.005$).

fold for L_{rigid}-LG and L_{fluid}-LG liposomes, respectively. The most efficient liposomes were L_{fluid}-LG, which increased transcytosis by more than 414% compared to ligand-free, rigid liposomes, transporting an amount of 111 pmol calcein into the basal media. This corresponds to 5.1% of the amount provided to the cells. The amount of calcein found in the basal medium was comparable to that found inside the barrier forming cells after 24 hours, indicating that about 50% of all calcein taken up by the cells were transported into the basal media. More than 10% of this calcein in the basal media was still encapsulated in the vesicles if ligand-free liposomes were transcytosed, while only less than 1% intact liposomes were measured using ligand-bearing liposomes (data not shown).

Pharmacokinetics and Biodistribution

These parameters were determined for drug containing L_{fluid}- and L_{fluid}-LG vesicles and compared to free MTO. All formulations were given at 5 mg/kg in a single intravenous dose. Content in samples were quantified using HPTLC as described in the Materials and Methods section.

Both liposomal formulations had a longer blood circulation time than the free drug (Fig. 5a). The liposomal drug could still be detected after 48 h, while the free drug could only be detected during first 5 h. There was no decisive difference in the brain concerning drug concentration after treatment with fluid ligand free and fluid ligand bearing liposomes (Fig. 5b).

A two-compartment model was used to simulate the plasma distribution over time after intravenous injection and to calculate the PK data shown in Table IV. All PK data demonstrated a clear advantage for the liposomal MTO.

We found for liposomal MTO a longer circulation time, it had a 12-fold larger AUC, a more than 10-fold longer clearance time, and a five-fold longer mean resistance time as compared to the free drug. This indicates that the liposomes had much better bioavailability than the free drug. No difference could be detected between the ligand-fee and ligand-bearing liposomal formulations.

The advantage for liposomal MTO was also found when drug concentration in different organs was quantified. Concentration *versus* time profiles for liver, lung, heart, kidney, spleen and subcutaneous tumor are shown in Figures S3–S8 in the Supplementary Material, while a summary reflecting the situation at 15 min after treatment is given in Figure S9 (Supplementary Material). The highest concentration of MTO was found in liver and kidney corresponding to more than 10% of applied dose. Liposomal MTO was found at higher concentrations than free MTO in liver by about 40% and in the spleen by 33–50%, while the opposite was found in the kidney, heart, and lung, where MTO concentration was reduced by 40%, 30–40%, and 33%, respectively, for the liposomal drug.

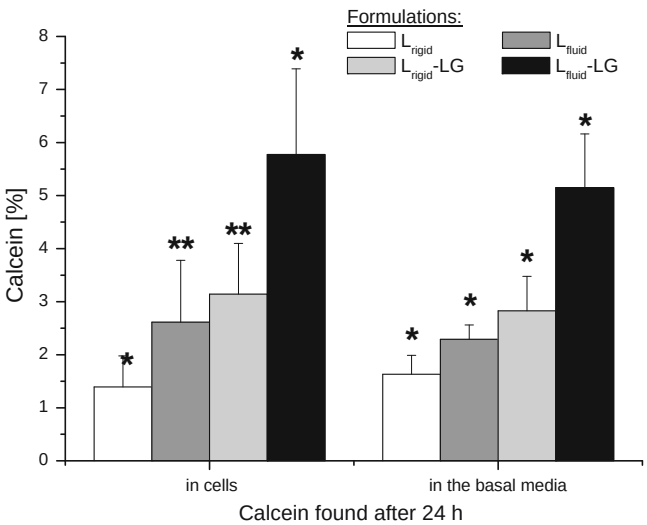

Fig. 4 Transcytosis of non-ligand and ligand bearing liposomes through a MDCK cell barrier. MDCK cells ($1*10^5$) were seeded on a permeable and collagen coated cell culture insert. Cells were incubated with 400 µl nutrient deficient DMEM containing liposomes (75 nmol TL/ml) in the apical chamber of the transwell system at 37°C for 24 h. After that time, the calcein concentration in the basal media and in cells was determined by fluorescence measurement directly (basal media) or after lysis (cells) as described in Materials and Methods. Three experiments were performed, each done in triplicate. *: Significantly different to all other values, **: Significantly different to all except to L_{rigid}-LG or L_{fluid}; ($p > 0.05$).

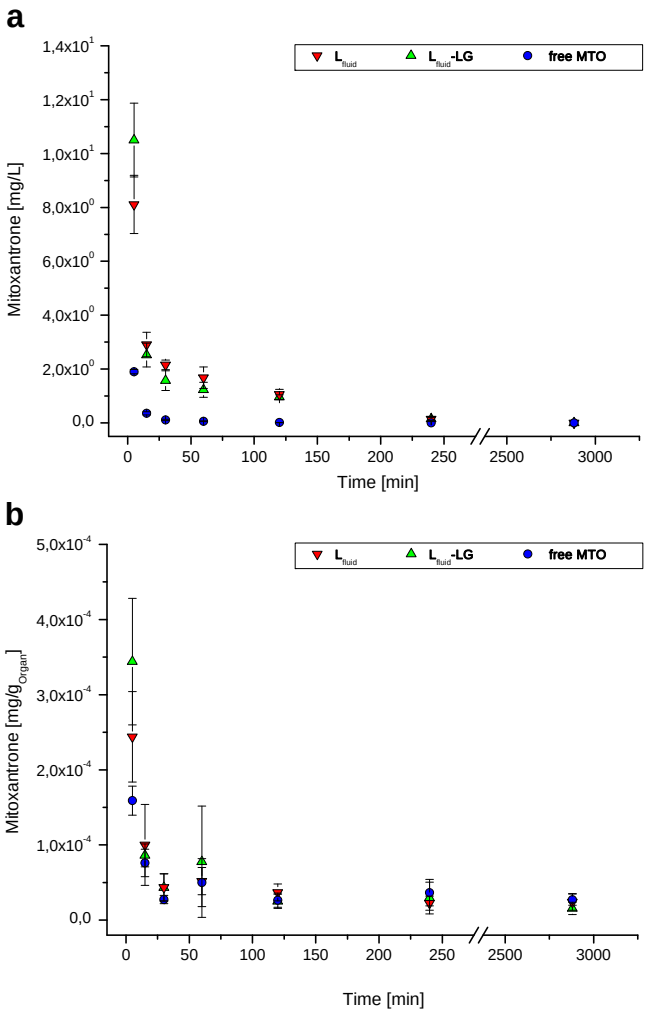

Fig. 5 Concentration versus time of free and liposomal MTO. NMRI:nu/nu mice were injected with 5 mg/kg MTO as solution or encapsulated in liposomes at $t=0$ and mice were sacrificed at pre-defined time points. MTO concentration was determined as described in Materials and Methods by HPLC. All data represent the mean ± S.D. for 3 samples, each determined in duplicate. (**a**) Plasma profile; (**b**) brain profile

The amount of MTO in the brain was 0.02–0.03% (Supplementary Material S9, insert) and maximum values were determined 5 min after injection with values of approximately $1.5*10^{-4}$ mg/g, $2.4*10^{-4}$ mg/g, and $3.4*10^{-4}$ mg/g for free MTO, $L4_{fluid}$, and $L4_{fluid}$-LG, respectively, indicating a clear grading from free drug, followed by liposomal drug to finally drug transported by ligand equipped liposomes.

Therapeutic Effect

Liposomes L_{rigid} and L_{fluid} without and with ligand were finally tested for their therapeutic effect in human MT-3 breast cancer xenografts growing in the brain of nude mice. Tumor cells were intracerebrally transplanted and additionally applied subcutaneously into the flank of the same mice to check the sensitivity of this tumor. Figure S10 (Supplementary Material) shows the relative tumor growth curve for the subcutaneous tumors after intravenous MTO-treatment. RTV of the treated to control group (T/C) were determined to be 31.2% and 11.9% at day 13 for MT-3 breast carcinoma, after treatment with free MTO or MTO in L_{fluid}-LG, respectively.

All formulations caused a significant inhibition of intracerebral tumor growth. Growth inhibition was calculated using the tumor area measured in brain cryosections of the mice, which are exemplified by the corresponding bars in Fig. 6. The inhibition was less pronounced than that seen with the subcutaneous tumor. With free MTO, an inhibitory effect (T/C RTV) of 50.9% was measured. The best result was obtained with L_{fluid}-LG with an inhibition of 72.9%, which was significantly better than free MTO ($p=0{,}002$) and also better than targeted rigid liposomes LG_{rigid}-LG ($p=0{,}094$). The formulation L_{fluid} without ligand was also more effective than free MTO and led to an inhibition of 64.1% ($p=0{,}007$).

Though all mice survived treatments, free MTO caused serious side effects manifested by significant but transient body weight loss of up to 36% (Figure S10) due to diarrhea and dehydration. The dehydration was also responsible for flaky skin observed in this group. All these side effects were markedly reduced in mice treated with liposome-associated MTO at the same dose.

DISCUSSION

A systemic treatment with anticancer drugs for primary and secondary brain tumors is still hampered because of the highly efficient blood–brain barrier, which prevents or reduces the transport of anticancer drugs into the brain. Only a few promising data from the literature are available (11). Beside the circumvention of the transport across the intact BBB, as it was shown for a locoregional treatment with MTO microspheres, which had a strong inhibitory effect on malignant gliomas (38,39), the transport itself can be improved. One

Table IV PK parameter for plasma distribution of MTO

Property[a]	Liposomes		
	Free MTO	L_{fluid}	L_{fluid}-LG
AUC [mg*h*L^{-1}] (±%)	0.54 (1.6)	6.38 (6.4)	6.18 (9.4)
$t_{1/2}$ [h] (±%)	0.08 (2.5)	0.21 (19.9)	0.15 (16.2)
Vd [L] (±%)	0.07 (9.7)	0.03 (9.1)	0.03 (15.9)
Cl [L/h] (±%)	0.23 (1.6)	0.02 (6.4)	0.02 (9.5)
MRT [h] (±%)	0.32 (11.1)	1.47 (14.0)	1.52 (24.1)

[a]: x (±%) - Given is the deviation of the calculated (bold) from the theoretical value based on the plasma distribution in a two compartment model after a single bolus injection of the drug in percent.

AUC: area under the curve; $t_{1/2}$: half life time; Vd: distribution volume; Cl: clearance; MRT: mean residence time.

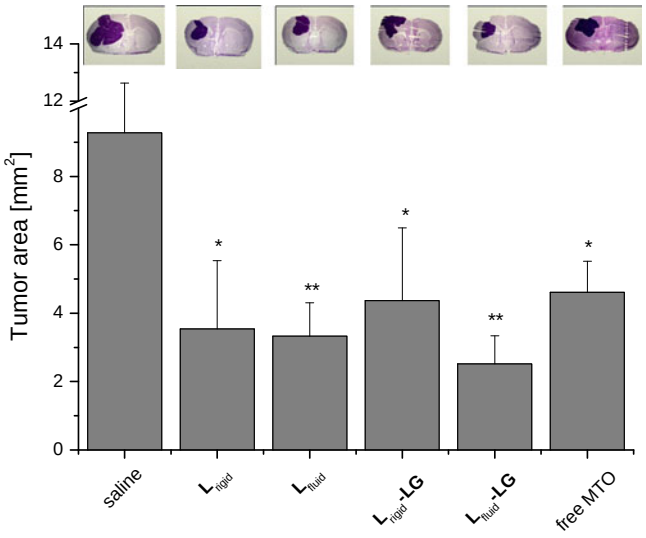

Fig. 6 Inhibition of brain tumor growth after treatment with different MTO formulations. MT-3 cells were transplanted s.c. into the left flank ($5*10^6$) and into the brain ($5*10^3$) of each nude mouse. Mice were treated i.v. with liposomes containing MTO or with free MTO, each in a dose of 4 mg/kg at day 3, 7 and 10. Control mice received saline solution. Diameter of subcutaneously growing tumor was measured twice weekly. Mice were sacrificed at day 22. Brains were isolated, snap-frozen and cryo-sections were prepared. The size of the tumor area was determined after tumor cell staining with cresyl violet by microscopic measurement. Top of figure shows pictures of cryo-sections of selected mice brains representing the mean area calculated for the complete treatment group shown in the bars. *: Significantly different to saline, **: significantly different to saline and to free MTO; ($p > 0.05$).

potential approach to transport drugs better across the BBB is their encapsulation into nanoparticles, which significantly changes the biophysical properties and the pharmacokinetic distribution of the drug decisively. So it could be demonstrated that doxorubicin loaded liposomes (Doxil, Caelyx) were very promising in clinical trials (40,41). Later, ligand equipped liposomes have been developed to target different receptors expressed (mainly) at the surface of the BBB, including the insulin-, transferrin, folate-receptors or others (for review see Orthmann 2011, (11)). On the other hand, to our knowledge, there are no reports on the application of LRP-targeted liposomes for the systemic treatment of brain malignancies.

Based on our previous findings *in vitro*, demonstrating that fluid membrane liposomes were best taken up and transcytosed by barrier forming MDCK cells, we assumed that a specific targeting of these liposomes to the LRP expressed on the surface of barrier forming cells may further enhance the transport across barriers such as the BBB by exploitation of an endocytotic pathway (2,30).

The basic concept of the current study was therefore to compare the most efficient fluid liposomes, L_{fluid}, with targeted fluid liposomes L_{fluid}-LG, which are equipped with a peptide ligand for specific targeting of the LRP. We used the anthracenedione MTO as anticancer drug because it poorly crosses the BBB but has a strong antitumor effect against mammary carcinomas like MT-3, which we wanted to use as an experimental brain metastasis model in our study.

We obtained the liposomes in a three-step process, starting with the preparation of MLV and their extrusion to obtain LUV, followed by the remote loading of MTO into the preformed LUV. This way to encapsulate MTO seems to be the method of choice, because it has been demonstrated that the remote loading is very effective in entrapping weakly amphiphilic bases (31) like doxorubicin (24), MTO (32), irinotecan (32), or vincristine (33). In the last step, the post insertion method (25) was applied to couple the 19-mer peptide at the surface of the preformed, MTO-loaded liposomes for targeting. This method requires only mild conditions which do not affect the drug loaded liposomes. After optimization of the individual preparation steps, liposomes were obtained which fulfilled the requirements for the intended *in vitro* and *in vivo* experiments concerning size, calcein (marker for *in vitro* experiments) or MTO (drug for *in vivo* experiments) loading and storage stability.

Functionality of liposomes was characterized *in vitro*. The first step and essential precondition for a successful transcytotic transport across a cell barrier is the cellular uptake. Comparing the uptake of calcein encapsulated in fluid and rigid, ligand-free liposomes in four different cell lines, the difference was only small or negligible for ligand-free liposomes, but a clear enhancement of uptake in the range of 2.6- (MDCK cells) to 9.2-fold (U373 cells) could be quantified if ligand equipped liposomes were used. The highest marker uptake was obtained with fluid-membrane, ligand bearing liposomes. That indicates that uptake is determined much more by the presence of a ligand inducing endocytosis as by vesicular membrane properties, inducing fusion (36) or adsorption (37) with the target cell membrane.

This was also confirmed in transcytosis experiments. The ability of the liposomes to cross cellular barriers by transcytosis was quantified as described recently (8) using a transwell system together with MDCK cells, which form a tight barrier between the apical and basal media layer, The tightness of the barrier was checked microscopically and by TER measurements and only wells with values greater $220\Omega*cm^2$ after background correction were used. Barrier tightness was also verified by inhibition of FITC dextran transport through the MDCK cell barrier.

As we recently reported (8), fluid vesicles were transcytozed to a higher amount than rigid liposomes. The insertion of the ligand enhanced transcytosis significantly, in comparison to the corresponding ligand-free liposomes. That corresponds to a transport across the cell barrier of 5% of the total amount of calcein added by the most efficient liposomes L_{fluid}-LG.

We assume that the results in transcytosis are caused by two different processes. Endocytosis seems to be more effective if it is receptor (LRP) mediated, which would explain the higher uptake of ligand equipped liposomes in comparison to non-modified ones. Transcytosis is also dependent on the stability of the liposomes. Fluid membrane liposomes are less stable

than rigid ones. A faster release of the liposomal content into the cytosol after cellular uptake provides more compound to the cell than from rigid liposomes. As it was already discussed recently (8), this free compound can be easily exocytosed again (e.g. into the basal compartment, or to the apical side of the BBB) or it is responsible for the higher cytotoxicity of MTO encapsulated into fluid membrane liposomes as it was described by Kawano *et al.* (42).

MTO-loaded fluid membrane liposomes without and with ligand were finally tested for their therapeutic effect in a xenograft brain metastasis model using human MT-3 breast cancer cells. This model was developed to mimic metastasis of primary breast tumor to the brain. Extensive experiments were performed to determine the optimum conditions for intracerebral tumor growth regarding cell number necessary for transplantation and growth rate. An additional s.c. transplantation of cells into the same mouse enabled the parallel measurement of the sensitivity of the MT-3 tumor against MTO. We found that the growth of the subcutaneous tumor could be almost completely inhibited by all MTO formulations. While targeted liposomes tended to be the best formulation, the difference in inhibition was not significant.

We used a schedule for the treatment, which started at day 3 after tumor cell inoculation when the tumors were still small, suggesting that the BBB is still intact at that early time point.

As a measure for growth inhibition, the tumor area was determined in serial cryosections of the mouse brains. The slice with the largest tumor area was selected and used for analysis. All formulations caused a significant inhibition of intracerebral tumor growth with an increase in inhibition from free MTO < ligand free liposomes < ligand bearing liposomes. The best result was obtained with targeted fluid liposomes, which were significantly more effective in tumor growth inhibition than free MTO (p=0.002) and also than the corresponding rigid liposomes (p=0.094). Both fluid liposomal formulations were significantly better than the free drug, but the difference between these liposomal formulations was not significant. This was also found in the PK study, where we determined the same drug concentrations in the brain for both types of liposomes and only found an enhancement of drug concentration compared with free MTO during the first minutes after treatment. The therapeutic results indicate that this increase in the drug concentration at a very early time point is apparently sufficient to cause the increase in antitumor efficacy.

A clear advantage of the liposomal MTO was also seen with respect to the reduction of side effects. Treatment with free MTO caused serious side effects manifested as significant body weight loss of up to 36% accompanied by diarrhea and dehydration, and the appearance of flaky skin. All these side effects were clearly reduced with the use of equal doses of MTO in liposomes, because of their improved biodistribution.

Taken together, our results show that fluid membrane liposomes clearly improve the therapeutic index of MTO. The advantage of targeted therapy using the angiopep-ligand was not as pronounced as expected from the report of Regina (21), which described a strong accumulation of paclitaxel in the brain of mice after perfusion if the drug was conjugated to angiopep (GRN1005, formerly ANG1005). On the other hand, the therapeutic effect they described for their mouse model was not very convincing, because an increase in lifespan of only 15–21% was observed. In a recent study comparing different ligands for brain targeting, it was found that liposomes equipped with angiopep were not taken up better than ligand free liposomes by human endothelial cells *in vivo* (43). In light of these reports, the improvement of the therapeutic index obtained with our targeted, fluid membrane liposomes are an important contribution to enhance the therapeutic potential of vesicular formulations targeting brain malignancies. Nevertheless, the targeting principle requires further investigation to enable optimization in its design and efficacy.

We are currently continuing in this research to develop more efficient Trojan Horse-like liposomes for the systemic treatment of malignant diseases in the central nervous system.

ACKNOWLEDGMENTS & DISCLOSURES

This project was financed in part by a grant of the Federal Ministry of Economics and Technology of Germany, PRO INNO II (KA0453401UL7). The authors gratefully acknowledge the excellent technical support of Annika Hoffmann (EPO GmbH, Berlin) and the valuable discussions about post insertion technology with Ronny Rüger (Friedrich-Schiller-Universität Jena). We also thank Lipoid GmbH Ludwigshafen for providing us with egg phosphatidylcholine.

REFERENCES

1. Abbott NJ, Patabendige AA, Dolman DE, Yusof SR, Begley DJ. Structure and function of the blood–brain barrier. Neurobiol Dis. 2010;37(1):13–25.
2. Pardridge WM. Preparation of Trojan horse liposomes (THLs) for gene transfer across the blood–brain barrier. Cold Spring Harb Protoc. 2010;(4) (2010), db.
3. Agarwal A, Lariya N, Saraogi G, Dubey N, Agrawal H, Agrawal GP. Nanoparticles as novel carrier for brain delivery: a review. Curr Pharm Des. 2009;15(8):917–25.
4. Blasi P, Schoubben A, Giovagnoli S, Rossi C, Ricci M. Lipid nanoparticles for drug delivery to the brain: *in vivo* veritas. J Biomed Nanotechnol. 2009;5(4):344–50.
5. Patel MM, Goyal BR, Bhadada SV, Bhatt JS, Amin AF. Getting into the brain: approaches to enhance brain drug delivery. CNS Drugs. 2009;23(1):35–58.
6. Tiwari SB, Amiji MM. A review of nanocarrier-based CNS delivery systems. Curr Drug Deliv. 2006;3(2):219–32.
7. Pardridge WM. Biopharmaceutical drug targeting to the brain. J Drug Target. 2010;18(3):157–67.
8. Orthmann A, Zeisig R, Koklic T, Sentjurc M, Wiesner B, Lemm M, *et al.* Impact of membrane properties on uptake and transcytosis of

colloidal nanocarriers across an epithelial cell barrier model. J Pharm Sci. 2010;99(5):2423–33.
9. Chamberlain MC. Anticancer therapies and CNS relapse: overcoming blood–brain and blood-cerebrospinal fluid barrier impermeability. Expert Rev Neurother. 2010;10(4):547–61.
10. Laquintana V, Trapani A, Denora N, Wang F, Gallo JM, Trapani G. New strategies to deliver anticancer drugs to brain tumors. Expert Opin Drug Deliv. 2009;6(10):1017–32.
11. Orthmann A, Fichtner I, Zeisig R. Improving the transport of chemotherapeutic drugs across the blood–brain barrier. Expert Rev Clin Pharmacol. 2011;4(4):465–78.
12. Cerletti A, Drewe J, Fricker G, Eberle AN, Huwyler J. Endocytosis and transcytosis of an immunoliposome-based brain drug delivery system. J Drug Target. 2000;8(6):435–46.
13. Boado RJ. Blood–brain barrier transport of non-viral gene and RNAi therapeutics. Pharm Res. 2007;24(9):1772–87.
14. McNeeley KM, Karathanasis E, Annapragada AV, Bellamkonda RV. Masking and triggered unmasking of targeting ligands on nanocarriers to improve drug delivery to brain tumors. Biomaterials. 2009;30(23–24):3986–95.
15. Feng B, Tomizawa K, Michiue H, Miyatake S, Han XJ, Fujimura A, *et al.* Delivery of sodium borocaptate to glioma cells using immunoliposome conjugated with anti-EGFR antibodies by ZZ-His. Biomaterials. 2009;30(9):1746–55.
16. Demeule M, Currie JC, Bertrand Y, Che C, Nguyen T, Regina A, Gabathuler R, Castaigne JP, Beliveau R. Involvement of the low-density lipoprotein receptor-related protein in the transcytosis of the brain delivery vector angiopep-2. J Neurochem. 2008;106 (4):1534–44.
17. Li Y, Cam J, Bu G. Low-density lipoprotein receptor family: endocytosis and signal transduction. Mol Neurobiol. 2001;23 (1):53–67.
18. Lillis AP, Van Duyn LB, Murphy-Ullrich JE, Strickland DK. LDL receptor-related protein 1: unique tissue-specific functions revealed by selective gene knockout studies. Physiol Rev. 2008;88(3):887–918.
19. Hussain MM, Strickland DK, Bakillah A. The mammalian low-density lipoprotein receptor family. Annu Rev Nutr. 1999;19:141–72.
20. Demeule M, Regina A, Che C, Poirier J, Nguyen T, Gabathuler R, Castaigne JP, Beliveau R. Identification and design of peptides as a new drug delivery system for the brain. J Pharmacol Exp Ther. 2008;324(3):1064–72.
21. Regina A, Demeule M, Che C, Lavallee I, Poirier J, Gabathuler R, *et al.* Antitumour activity of ANG1005, a conjugate between paclitaxel and the new brain delivery vector Angiopep-2. Br J Pharmacol. 2008;155(2):185–97.
22. Che C, Yang G, Thiot C, Lacoste MC, Currie JC, Demeule M, *et al.* New Angiopep-modified doxorubicin (ANG1007) and etoposide (ANG1009) chemotherapeutics with increased brain penetration. J Med Chem. 2010;53(7):2814–24.
23. Chan WC, White PD. Fmoc solid phase peptide synthesis – A practical Approach. Oxford: Oxford University Press; 2000.
24. Fritze A, Hens F, Kimpfler A, Schubert R, Peschka-Süss R. Remote loading of doxorubicin into liposomes driven by a transmembrane phosphate gradient. Biochim Biophys Acta. 2006;1758 (10):1633–40.
25. Gantert M, Lewrick F, Adrian JE, Rossler J, Steenpass T, Schubert R, *et al.* Receptor-specific targeting with liposomes *in vitro* based on sterol-PEG(1300) anchors. Pharm Res. 2009;26(3):529–38.
26. Zeisig R, Müller K, Maurer N, Arndt D, Fahr A. The composition-dependent presence of free (micellar) alkylphospholipid in liposomal formulations of octadecyl-1,1-dimethyl-piperidino-4-yl-phosphate affects its cytotoxic activity *in vitro*. J Membr Biol. 2001;182(1):61–9.
27. Naundorf H, Fichtner I, Saul GJ, Haensch W, BÜttner B. Establishment and characteristics of two new human mammary carcinoma lines serially transplantable in nude mice. J Cancer Res Clin Oncol. 1993;119(11):652–6.
28. Johnson JL, Ahmad A, Khan S, Wang YF, Abu-Qare AW, Ayoub JE, *et al.* Improved liquid chromatographic method for mitoxantrone quantification in mouse plasma and tissues to study the pharmacokinetics of a liposome entrapped mitoxantrone formulation. J Chromatogr B Analyt Technol Biomed Life Sci. 2004;799 (1):149–55.
29. Diehl KH, Hull R, Morton D, Pfister R, Rabemampianina Y, Smith D, *et al.* A good practice guide to the administration of substances and removal of blood, including routes and volumes. J Appl Toxicol. 2001;21(1):15–23.
30. Pflanzner T, Janko MC, André-Dohmen B, Reuss S, Weggen S, Roebroek AJ, Kuhlmann CR, Pietrzik CU. LRP1 mediates bidirectional transcytosis of amyloid-beta across the blood–brain barrier. Neurobiol Aging. 2011;32(12):2323e1-11.
31. Gubernator J, Chwastek G, Korycinska M, Stasiuk M, Grynkiewicz G, Lewrick F, *et al.* The encapsulation of idarubicin within liposomes using the novel EDTA ion gradient method ensures improved drug retention *in vitro* and *in vivo*. J Control Release. 2010;146(1):68–75.
32. Ramsay E, Alnajim J, Anantha M, Zastre J, Yan H, Webb M, Waterhouse D, Bally M. A novel liposomal irinotecan formulation with significant anti-tumour activity: use of the divalent cation ionophore A23187 and copper-containing liposomes to improve drug retention. Eur J Pharm Biopharm. 2008;68(3):607–17.
33. Zucker D, Barenholz Y. Optimization of vincristine-topotecan combination–paving the way for improved chemotherapy regimens by nanoliposomes. J Control Release. 2010;146(3):326–33.
34. Ishida T, Harashima H, Kiwada H. Liposome clearance. Biosci Rep. 2002;22(2):197–224.
35. Zeisig R, Eue I, Kosch M, Fichtner I, Arndt D. Preparation and properties of sterically stabilized hexadecylphosphocholine (miltefosine)-liposomes and influence of this modification on macrophage activation. Biochim Biophys Acta. 1996;1283(2):177–84.
36. Xi X, Yang F, Chen D, Luo Y, Zhang D, Gu N, *et al.* A targeting drug-delivery model via interactions among cells and liposomes under ultrasonic excitation. Phys Med Biol. 2008;53(12):3251–65.
37. Torchilin VP. Recent approaches to intracellular delivery of drugs and DNA and organelle targeting. Annu Rev Biomed Eng. 2006;8:343–75.
38. Bhaskar S, Tian F, Stoeger T, Kreyling W, de la Fuente JM, Grazu V, Borm P, Estrada G, Ntziachristos V, Razansky D. Multifunctional Nanocarriers for diagnostics, drug delivery and targeted treatment across blood–brain barrier: perspectives on tracking and neuroimaging. Part Fibre Toxicol. 2010;7(3):3. doi:10.1186/1743-8977-7-3.
39. Yemisci M, Bozdag S, Cetin M, Soylemezoglu F, Capan Y, Dalkara T, *et al.* Treatment of malignant gliomas with mitoxantrone-loaded poly (lactide-co-glycolide) microspheres. Neurosurgery. 2006;59 (6):1296–302.
40. Boiardi A, Eoli M, Salmaggi A, Lamperti E, Botturi A, Broggi G, *et al.* Systemic temozolomide combined with loco-regional mitoxantrone in treating recurrent glioblastoma. J Neurooncol. 2005;75(2):215–20.
41. Boiardi A, Eoli M, Salmaggi A, Lamperti E, Botturi A, Solari A, *et al.* Local drug delivery in recurrent malignant gliomas. Neurol Sci. 26 2005; Suppl 1(S37–9):S37–S39.
42. Kawano K, Onose E, Hattori Y, Maitani Y. Higher liposomal membrane fluidity enhances the *in vitro* antitumor activity of folate-targeted liposomal mitoxantrone. Mol Pharm. 2009;6(1):98–104.
43. van Rooy I, Mastrobattista E, Storm G, Hennink WE, Schiffelers RM. Comparison of five different targeting ligands to enhance accumulation of liposomes into the brain. J Control Release. 2011;150 (1):30–6.
44. Zeisig R, Koklic T, Wiesner B, Fichtner I, Sentjurc M. Increase in fluidity in the membrane of MT3 breast cancer cells correlates with enhanced cell adhesion *in vitro* and increased lung metastasis in NOD/SCID mice. Arch Biochem Biophys. 2007;459(1):98–106.